ap

Available on
www.asianjournalofphysics.in

Asian Journal of Physics Vol. 24, No 10 (2015) 1339-1354

Interferometry with broadband light: Applications in metrology

Mahendra Prasad Kothiyal[1] and Paul KumarUpputuri[2]

[1]*Superannuated from the Applied Optics Laboratory,*
Department of Physics, Indian Institute of Technology Madras- 600 036, India
[2]*School of Chemical and Biomedical Engineering,*
Nanyang Technological University, Singapore 637459

Dedicated to Padma Shri Prof R S Sirohi, FNAE

A broadband light interference pattern provides phase information corresponding to a range of wavelengths simultaneously. In the recent times a variety of applications such as 3D surface profiling, film thickness measurement, dispersion measurement, optical coherence tomography, long length metrology have been developed by extracting the phase information from the interferogram. Some of these procedures have been reviewed here. © Anita Publications. All rights reserved.

Keywords: Interferometry, Broadband light, Interferogram, Fourier transform, Super Luminescent Diode (SLD).

1 Introduction

A broadband light produces a spectacular coloured interference pattern. Interference in the films produced by the sunlight has always been fascinating. The credit for an early application of white light fringes goes to A Michelson. In the recent times several applications of broadband light interference have been investigated [1-23]. One may look at the interferogram due to a broadband source as an incoherent superposition of large number of monochromatic interferograms. This superposition results in a unique intensity distribution in the interferogram with a maximum at zero path difference such that the identification of equality of path difference in the two arms of an interferometer becomes a simple matter. This equality of path difference is extensively used for profiling applications by locating this maximum. In fact Michelson used this principle in 1881 in one of the pioneering experiment using interference of light for the calibration of a standard meter. In yet another approach to get useful information from a white light interferogram is to decompose in its individual constituents, which may be accessed at the output of a spectrograph, if the interferogram is imaged at the entrance slit of the spectrograph [14-24]. The broadband source interference signal may also be Fourier transformed to get the individual monochromatic components [11]. An important advantage of a broadband light source is that it can overcome the ambiguity problem associated with monochromatic interferometry. In a broadband light source such, as a filament lamp (white light) or Super Luminescent Diode (SLD), a range of wavelengths are simultaneously present. Alternatively, the broad band effect can also be achieved by the use of lasers at multiple wavelengths, tunable diode laser (swept source), or color CCD camera or a 3 chip color CCD camera used with white light.

Extraction of useful information from an interferogram requires careful fringe analysis, techniques that are fast and can be automated. This is important from the point of view of eliminating errors. The development of fringe analysis techniques has played an important role in improving the resolution and accuracy. Procedures such, as temporal and spatial phase shifting technique, heterodyne interferometry, Fourier and Hilbert transform techniques have been employed. Phase shifting has been the most used approach. Temporal phase shifting most frequently makes use of a PZT to introduce phase shift. Polarization phase shifting is another useful method of producing phase shift between the interferograms. This allows acquisition of multiple phase shifted frame in single shot and hence allows measurements even in dynamic environments. Polarization phase shifting technique has recently been found very useful in this respect [13].

Corresponding author :
*e-mail:*mpkothiyal49@gmail.com (Mahendra Prasad Kothiyal)

The other possibility is the use of color CCD with its three channels. In the following sections, we review various interference measurement techniques using broadband light.

2 Interference with broadband light

A broadband light source has a small coherence length, the actual value depending on the bandwidth. For white light source such as a tungsten halogen lamp, it is in the range of a few micrometers. The fringes localize in the vicinity of the test object when the paths between the test and measurement arms of an interferometer match closely. The contrast of the fringes is a maximum here. In other words, the fringe contrast function (coherence envelope) peaks at zero path difference.

2.1 Interference Equation

For a broadband light source the intensity distribution in the interference pattern is given by the equation [4]

$$I = I_r + I_t + 2\sqrt{I_r I_t}\ \gamma^r_{11}(\tau) \quad (1)$$

where I_r and I_t are respectively the intensities of the reference and test beams of the interferometer. $\gamma^r_{11}(\tau)$ is the real part of $\gamma_{11}(\tau)$, the complex degree of coherence of the light source, and τ is the time delay between the two optical paths. A broadband light source may be assumed to have a Gaussian power spectral density function. The value of $\gamma_{11}(\tau)$ is given by

$$\gamma_{11}(\tau) = \exp[-(\pi\tau\Delta\nu)^2]\exp(-i2\pi\bar{\nu}\tau) \quad (2)$$

where $\bar{\nu}$ is the central frequency and $\Delta\nu$ is the spectral width. Equation (1) can be rewritten as

$$I = I_r + I_t + 2(I_r\, I_t)^{1/2}\, g(z)\cos(\phi(z) + \phi_0) \quad (3)$$

where $g(z) = \exp[-(\pi\tau\Delta\nu)^2]$ is the coherence envelope or the fringe contrast function and $\phi(z) = 2\pi\bar{\nu}\tau$, and ϕ_0 is the phase shift which accounts for phase changes such as phase shift on reflection. In Eq (3), $2z$ is the round trip path difference suffered by the interfering beam in a double pass interferometer such as Michelson, Linnik or Mirau in which the actual difference of the arm lengths from the beam splitters is z. z is related to τ as $\tau = 2z/c$; hence

$$\phi(z) = \frac{2\pi}{\bar{\lambda}}(2z) \quad (4)$$

Equation (3) can be rewritten as

$$I = I_0\,(1 + G(z)\cos\phi(z)) \quad (5)$$

where $G(z) = Vg(z)$, $I_0 = I_r + I_t$ and $V = 2\sqrt{(I_r\, I_t)}/I_0$, V is the visibility or contrast. The simulated intensity variation

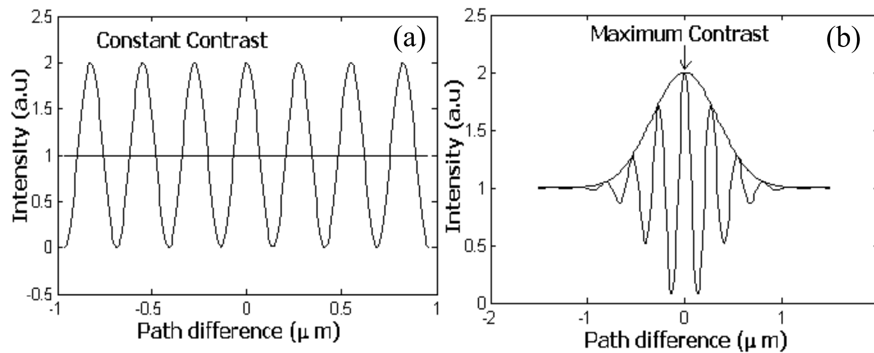

Fig 1. Simulated intensity variation in fringe systems, (a) Monochromatic light, (b) White light

with z calculated using Eq (3) is shown in Fig 1(b) for $\phi_0 = 0$. Figure 1(a) on the other hand shows simulated fringe pattern for monochromatic light for which $\Delta\nu = 0$ and $G(z) = 1$. The envelope in Fig 1(b) is the fringe contrast or the visibility curve and has peak at $z = 0$. The fringe contrast decreases rapidly as the path difference is increased from zero. The peak of the fringe contrast function (the correlation peak) represents zero path difference condition between the object and reference beams. This capability of a white light interferometer to show the zero path condition without any phase ambiguity, as against a monochromatic interferogram, where same value of maximum and minimum repeats itself, is of great value in optical metrology with broadband light. For non-zero value of ϕ_0 the, the maximum of the fringe pattern within the envelop is not at $z = 0$. Figure 2 shows actual interferograms with white light and laser light recorded over a surface with step. Figure 2(c) is a white light interferogram taken by a black and white camera. Figure 3 shows typical intensity scans of actual laser and white light interferograms.

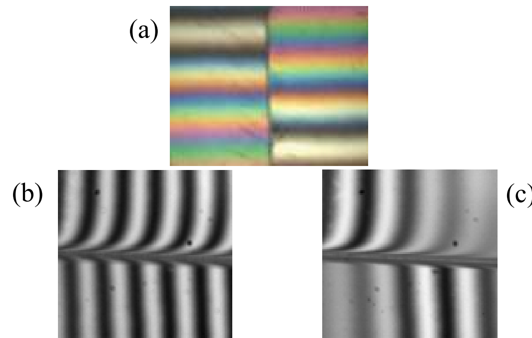

Fig 2. Interferograms of step objects: (a) white light interferogram; (b) laser light interferogram; (c) white light interferogram taken with black and white camera.

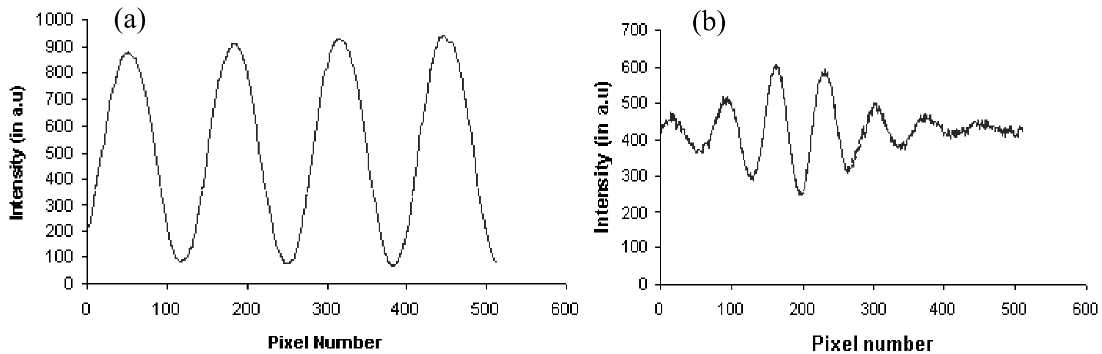

Fig 3. Intensity Scans of (a) monochromatic light interferogram, (b) white light interferogram.

2.2 Monochromatic fringe analysis using phase shifting interferometry (PSI)

In the process of analyzing broadband interference, we need to analyze monochromatic fringe patterns as well in some procedures. Here we discuss how monochromatic interferograms are evaluated using phase shifting methods. For monochromatic light the Eq (5) can be written as

$$I(x,y) = I_0(x,y)\ \{1+ V(x,y)\ \cos[\phi(x,y)+ \alpha]\} \tag{6}$$

where $G(z) = V$ as $g(z) = 1$ for monochromatic illumination and ϕ_0 is assumed zero. In PSI the phase of one of the arms of the interferometer is shifted in steps α and the new intensity at various points (x,y) in the interferogram is recorded at each step.

There are several algorithms available to determine $\phi(x,y)$ and $V(x,y)$ from Eq (6) [24,25]. Since there are three unknowns in Eq (6), a minimum of three interferograms is required to solve for the wavefront phase and contrast. With steps being –α, 0 and α, Eq (6) can be solved for the unknown wavefront phase as

$$\phi(x,y) = \tan^{-1}\left\{\frac{1-\cos\alpha}{\sin\alpha}\left(\frac{I_1 - I_3}{2I_2 - I_1 - I_3}\right)\right\} \tag{7}$$

There are however several errors compensating algorithms that are less sensitive to reference phase shift calibration and other errors [8,25,26]. A five step algorithm with phase shift values as –2α, –α, 0, α, 2α with α,usually being close to π/2, gives

$$\phi(x,y) = \tan^{-1}\left\{2\sin\alpha\left(\frac{I_2 - I_4}{2I_3 - I_5 - I_1}\right)\right\} \tag{8}$$

$$\sin^2\alpha = \frac{4(I_2 - I_4)^2 - (I_1 - I_5)^2}{4(I_2 - I_4)^2} \tag{9}$$

The visibility (contrast function) is given as

$$V(x,y) = \frac{[4(I_2 - I_4)^2 + (2I_3 - I_1 - I_5)^2]^{1/2}}{I_1 + 2I_3 + I_5} \tag{10}$$

3 Scanning white light interferometry (WLI)

Figure 4 shows a microscope-based version of a broadband light interferometer. It is configured as a spectral interferometer discussed later. For scanning WLI the CCD will be placed at the ES plane (the entrance slit of the spectrometer). The scanning white light interferometer for surface metrology commonly makes use of a Mirau interference objective to scan the object [8]. Broadband light from a halogen lamp is directed to the objective. The objective is mounted on a piezoelectric translator (PZT) to translate the objective along the optical axis. The interferogram is imaged on to a CCD camera. Each frame is transferred to the host computer, which performs the acquisition and analysis functions and controls the PZT scan rate.

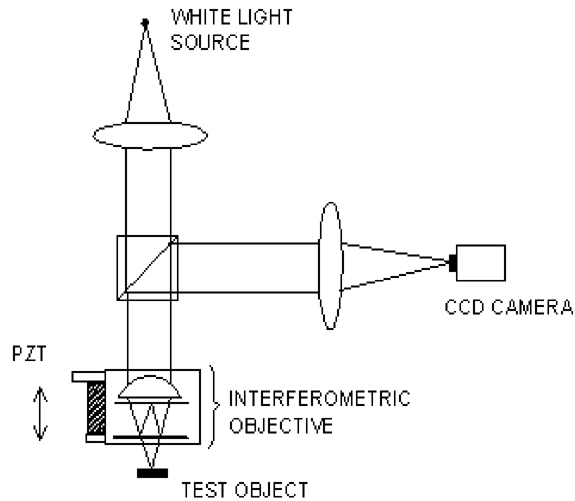

Fig 4. Scanning white light interferometer.

The Mirau objective has the disadvantage that it requires long working distance microscope objectives to accommodate the two plates, which consists of the reference surface and the beam splitter plate. A Linnik interference microscope can be used to avoid this difficulty [8]. If the PZT is moved in a continuous manner the output at any pixel will go through the sequence as shown in the Fig 1. Signal processing can be carried out to determine the peak position as a function of the scan position *z*. This is usually possible when measurement along *z*-axis alone is required as done in optical coherence tomography (OCT) as discussed later. To get a 3D picture $z(x,y)$ as in surface metrology, the scanning along the *z* axis is done in steps. In practice the PZT is moved in steps (usually $\bar{\lambda}/8$ where $\bar{\lambda}$ is the mean wavelength) starting from some reference position and data is available at discrete frame positions.

3.1 Computation of coherence envelope by phase shifting technique

It has been shown in Sec 2.2 that PSI can be used to determine both the phase and the fringe contrast (visibility). The fringe contrast is practically constant in monochromatic interferometry and its calculation is not of much interest. The white light interference pattern is expressed by Eq (3) in which $g(z)$ is the fringe contrast function which is not constant but varies with *z*, the scan position. The application of phase shifting technique to determine the fringe contrast function of a white light interferogram poses problems if the commonly used phase shifting method of translating the reference mirror with PZT is used. Firstly, the phase shift is not same for all the wavelengths. Secondly $g(z)$, the quantity to be determined is not same for all the steps. This will lead to error in the measurement. Nevertheless the phase shifting technique has been applied to white light interferometry using PZT phase shifter, as well as, the phase shifters based on polarization components, which can be made achromatic [13].

A successful error compensating 5-step algorithm is by Larkin [10] .Using this algorithm, the fringe contrast function $G(z)$ is given by

$$2G(z)\sin^2\alpha = [(I_2 - I_4)^2 - (I_1 - I_3)(I_3 - I_5)]^{1/2}/I_0 \quad (12)$$

For α close to $\pi/2$ for the central wavelength, $\sin^2\alpha/2 \approx 1$ and $G(z)$ can be evaluated by

$$G(z) = [(I_2 - I_4)^2 - (I_1 - I_3)(I_3 - I_5)]^{1/2}/2I_0 \quad (13)$$

In this equation, I_3 represents the intensity of the central frame ($\alpha = 0$). This algorithm by far gives the best agreement with the ideal coherence envelope.

4 Frequency Domain WLI

We may think of the scan history of the intensity modulation for an individual pixel in a white light interferogram as a sum of single wavelength (monochromatic) fringe patterns superposed incoherently one upon other [5]. The output intensity for a monochromatic constituent of wavelength λ can be expressed as (Eq (3) with $g(z) = 1$)

$$I(z, \lambda) = I_r + I_s + 2(I_r I_s)^{1/2}\cos[\phi(\lambda) + \phi_0] \quad (14)$$

where

$$\phi(\lambda) = \frac{4\pi z}{\lambda} \quad (15)$$

and ϕ_0 may be any additional phase shift for a given *z*. We may write, $\sigma = 1/\lambda$ then $\phi(\sigma) = 4\pi\sigma z$. The variation in $\phi(\sigma)$ with σ is linear and *z* may be obtained by a slope calculation if $\phi(\sigma)$ can be determined for a series of σ values, i.e.

$$z = \frac{\Delta\phi(\sigma)}{4\pi\Delta\sigma} \quad (16)$$

Each fringe pattern constituting the broadband light interferogram has a unique magnitude, phase and spatial frequency or wave number k defined here as the rate of change of phase with scan position. Peak fringe

contrast occurs at a scan position for which the phases of these constituent patterns all agree. Knowledge of the relative phases of the patterns at any given position in the scan tells as where we are with respect to the zero position. The information about the magnitude and phase ϕ of each constituent pattern can be extracted mathematically by means of a Fourier transform of scan history of the white light interference pattern [11].

The normalized Fourier transform of the intensity $I(z)$ is given by

$$P(k) = \int_{-\infty}^{\infty} I(z)\ exp(-ikz)dz \tag{17}$$

In practice at any pixel intensity values I_i taken at equally spaced OPD positions z_i during scanning. The Fourier transform of the scanned intensity may be represented as

$$P_j = |P_j| \exp(-i\phi_j) \tag{18}$$

The transformed interferogram now represents for each pixel, relative strength $|P_j|$ and interferometric phase ϕ_j corresponding to the constituent wave of white light having the wave number k_j. The phase is given by

$$\phi_j = \tan^{-1}\{Im(P_j)/Re(P_j)\} \tag{19}$$

As seen earlier the slope of the $(\varphi - k)$ line gives the local height z. The modulus of P_j represents the coherence envelope of the white light interferogram. The region where $|P_j|$ is large has the most useful information. This region in the FT data can be identified and a series of pairs (ϕ_j, k_j) from this region used for obtaining $(\phi_j - k_j)$ least square linear fit whose slope gives z. For the least square fit the phase data is weighted by $|P_j|^2$. The modulo 2π ambiguities in the phase data are removed by an unwrapping procedure.

5 Spectral Interferometry

The white light interferogram can be spectrally decomposed (Spectrally Resolved White Light Interferometry, SRWLI) by a spectrometer, which will produce a series of N monochromatic intensities modulated by a cosine function as described by Eq (18). The number N is determined by the number of pixels in the detection unit such as a CCD array. Each pixel along the chromaticity axis (the direction of dispersion) corresponds to a different σ. The aim is to determine $\phi(\sigma)$ at each pixel and use Eq (20) to determine z. These values can be extracted at each pixel (σ value) by Fourier transform technique [17] or by phase shifting technique [12,17]. In phase shifting technique one may use spatial phase shifting or temporal phase shifting.

5.1 Temporal phase shifting with PZT phase shifter

For a white light source a phase shift of $\pi/2$ with a PZT can be exact at only one wavelength such as the mean wavelength of the source. In SRWLI, in which interferogram are obtained over a range of wavelength, the phase shift will vary with the wavelength. Nevertheless a PZT phase shifter performs remarkably well in SRWLI in spite of its poor achromaticity. It has been seen that the errors introduced in the calculation of phases as a function of wavelength is oscillatory in nature and get averaged out when ϕvs. σ line is obtained from a least square fit [18]. Further, the magnitudes of the error is quite small with error compensating algorithms such as Eq (8) and practically zero with Eq (21).

5.2 Experimental Setup

The experimental setup to carry out surface profiling and film thickness measurement is shown in Fig 5. The test surface is observed through a Mirau-type interferometric microscope objective. The light source is a halogen lamp, which presents a broad continuous spectrum. At the exit plane of the microscope, the white-light interferogram of the surface is passed through the entrance slit (ES) of a direct-vision spectroscope. The ES selects a line of the test surface for profiling. The output of the spectroscope is received on a CCD camera. The camera is aligned such that the ES is parallel to the columns of pixels, so that the rows represent the chromaticity axis because the dispersion is perpendicular to the slit. To implement the phase shifting

technique the objective mount is fitted with a PZT. The camera (Pulnix 1010) gives a 10-bit digital output. The interferograms are transferred to the PC through an image acquisition board (NI PCI 1422). The control voltage to shift the PZT for phase shifting is produced by a digital to analog card (NI DAQ). For calibration of the CCD camera we used the cadmium (Cd) spectral lamp [19] .

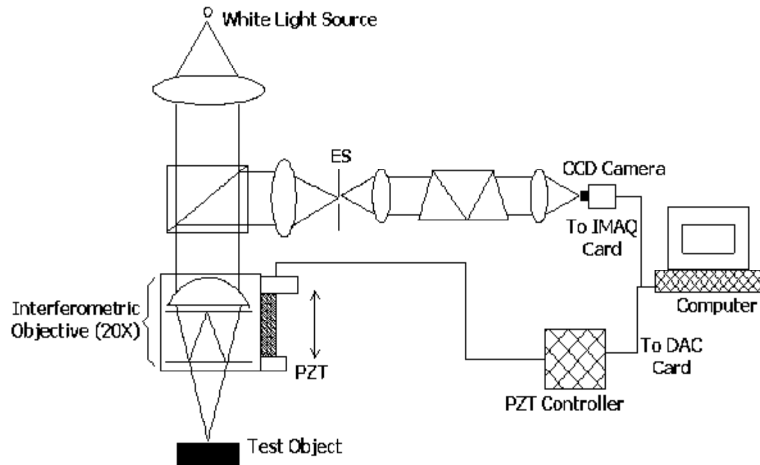

Fig 5. Schematic of a spectral interferometer

5.2.1 Experimental Results

5.2.1.1 Surface profiling

For this application the phase $\phi(\sigma)$ varies linearly with wave number σ as

$$\phi(\sigma) = 4\pi\sigma z \tag{20}$$

where $2z$ is the round trip optical path difference and is related to the surface height. The surface height z can be obtained from Eq(16).

For the calculation of phase $\phi(\sigma)$ we used the temporal phase shifting interferometry. In order to avoid phase calculation error due to the phase shift error at wavelength other than the mean wavelength, we have used the error compensating eight-step algorithm given by [24]

$$\tan\phi = \frac{-I_1 - 5I_2 + 11I_3 + 15I_4 - 15I_5 - 11I_6 + 5I_7 + I_8}{I_1 - 5I_2 - 11I_3 + 15I_4 - 11I_6 - 5I_7 + I_8} \tag{21}$$

where $I_1, I_2 \ldots\ldots I_8$ are the phase shifted spectral interferogram. Figure 4 shows the spectral interferogram of a plane surface, which is observed through the experimental setup shown in Fig 3. In the fringe pattern any cyclic variation of intensity along the chromaticity (horizontal) axis is due to phase difference as a result of wavelength change only. Similarly any variation in intensity along the vertical axis is due to change in optical path (due to air wedge, for example) as the wavelength is constant along any column of pixels. In any other arbitrary direction, there is contribution due to both. Eight such phase-shifted interferograms are needed to calculate the phase $\phi(\sigma)$.

The height value z determined from Eq (16) is less precise. This value of z is used as a first approximation to the true value and can be improved with the help of the available more precise monochromatic phase value using the equation given by [12,15,19,20],

$$z' = \frac{1}{4\pi\sigma}\left[\phi' - 2\pi\,\mathrm{int}\left(\frac{\phi' - 4\pi\sigma z}{2\pi}\right)\right] \tag{22}$$

where int (x) rounds offs to the nearest integer to x and z' is the improved value. The nearest integer determines

the fringe order. Figure 4 shows the line profile of a 1.76 μm standard step obtained using Eq (22). The step height was found to be (1761 ± 2) nm

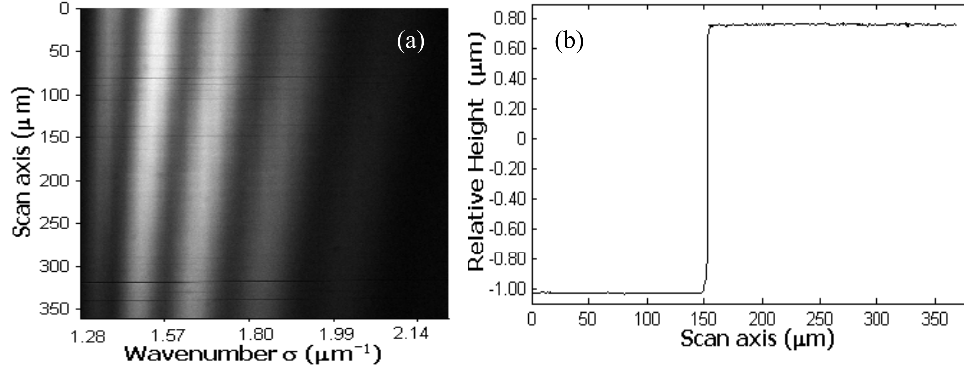

Fig 4. (a) A typical spectral interferogram, and (b) line profile of a 1.76 μm Standard step.

5.2.1.2 Film Thickness Profiling

When a transparent film is deposited on a substrate as shown in Fig 5, the reflection coefficient of the system is given by [21,22]

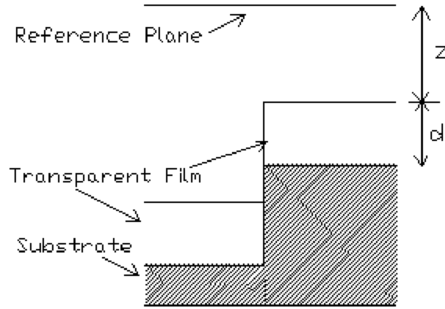

Fig 5. Cross section of a patterned surface and the substrate.

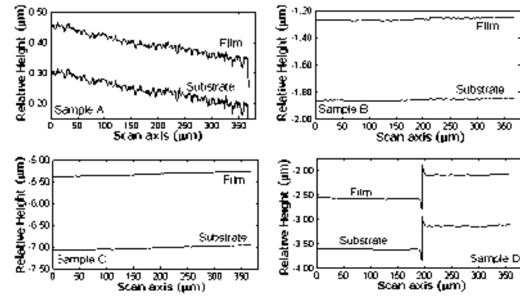

Fig 6. Line profiles of the top surface of the film.

$$R = \frac{r_{01} + r_{12}\exp(-i2\beta)}{1 + r_{01}r_{12}\exp(-i2\beta)} \quad (23)$$

where r_{01} and r_{12} represent the Fresnel reflection coefficients of the top and bottom surfaces of the film respectively, and β is given by the relation $\beta = 2\pi\sigma d n_2$, where d and n_2 are the thickness and refractive index of the transparent film, respectively. The reflection coefficient R is complex. The reflected beam due to the presence of the film, therefore, has a phase ψ.

The phase ϕ(σ) in this application can be written as [21,22]

$$\phi(\sigma) = 4\pi\sigma z + \psi(\sigma, d, n_2) \quad (24)$$

Since $\psi(\sigma, d, n_2)$ is a function of thickness d, ϕ(σ) is also a function of d. The first term (4πσz) on the RHS of Eq (24) is due to the air gap between the reference plane and the top of the transparent film. For the determination of surface height *z* and film thickness d we used the measured value of $\phi_{measured}(\sigma)$ to minimize the error function

$$\eta(z,d) = \sum\left[\phi_{model}(\sigma,z,d) - \phi_{measured}(\sigma)\right]^2 \quad (25)$$

for a particular value of z and d, where σ_c and $\Delta\sigma$ are the central wave number and the bandwidth of the white light source.

Experiment was carried out by recording fringes on a patterned silicon wafer on which a SiO_2 film has been deposited. The phase at a series of points along the wave number axis was determined and used to determine the surface height and the thickness of the layer at each point, as given by Eq (24), were then modeled so as to minimize the error function η given by Eq (25). Initially we used a linear fit to the experimental data, the slope of this phase $\phi(\sigma)$ vs. wave number line gives us an approximate value of (z + n_2d) since (z + n_2d) = slope / (4π). We then used the Levenberg–Marquardt nonlinear least squares fitting algorithm (Matlab) for thickness modeling. This algorithm requires an initial guess for d and z, which we can get from the above calculation. With these values of d, z and the refractive index as inputs, we obtain, as the output, independently adjusted values of d and z, which yield the best fit to the experimental values of the phase. Figure 6 shows film and substrate profiles obtained for the top surface of the film and the substrate for the sample used.

5.2.1.3 GVD measurement

In the presence of a dispersive sample in one arm of the interferometer such as a Michelson interferometer shown in Fig 7, the phase vs. wave number curve shows a stationary point as shown in Fig 9. At the stationary point the phase $\phi(\sigma)$ is quadratic with σ and is given by [23,26-28]

$$\phi(\sigma) = 4\pi^2 L k'' c^2 (\sigma - \sigma_0)^2 = A\sigma^2 + B\sigma + C \tag{26}$$

where L is the thickness of the sample, c is the velocity of the light and k″ is the group velocity dispersion (GVD) of the sample at $\sigma = \sigma_0$, which can be written as

$$k' = \frac{\lambda_0^3}{2\pi c^2} \frac{d^3 n}{\lambda_0^2} \tag{27}$$

where n is the refractive index of the sample. From Eqs (26) and (27), we have $\sigma_0 = -B/2A$ and $d^2n/d\lambda^2 = -B^3/16LA^2$. It can be clearly seen from Eqs (26) and (27) that, knowing the sample thickness L and the quadratic fit coefficients A, B, and C from the $\phi(\sigma)$ vs. σ plots, we can calculate the GVD ($\propto d^2n/d\lambda^2$) of the sample at any wavelength within the lamp spectrum.

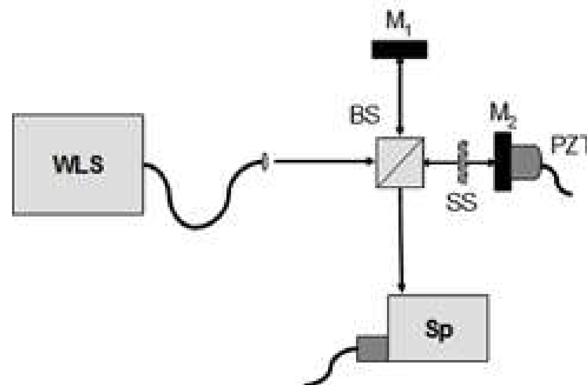

Fig 7. Schematic of the experimental setup for GVD measurement of a plate sample (SS).

To demonstrate the effectiveness of this technique for fast and accurate measurement of GVD we inserted a 1.60 mm thick silica glass slide in the sample arm of the interferometer shown in Fig 7. Figure 8 shows one of the spectral interferogram with the sample. Using Eq (21) we calculate the spectral phase. A

line scan of the phase $\phi(\sigma)$ versus σ around the stationary phase point σ_0 is shown in Fig 9 (trace b). We can displace the stationary point along the σ axis by appropriately delaying the interferometer arm and obtain a new phase $\phi(\sigma)$ versus σ for around a different σ_0 along the chromaticity axis. Figure 9 shows the line scans of the phase plots around different stationary points. Applying a quadratic fit to each curve and using Eqs (26) and (27), we calculated $d^2n/d\lambda_0^2$ for the corresponding $\lambda = \lambda_0$. Figure 10 shows the values of $d^2n/d\lambda_0^2$ as a function of wavelength of the silica sample. The curve in the figure is a theoretical curve calculated using the Sellmeier dispersion equation with experimental points shown on it by circles. The arrangement like Fig 7 can as well be used for refractometry of liquid samples, measurement of dispersion curves, or effective thickness of samples with known dispersion [26-28].

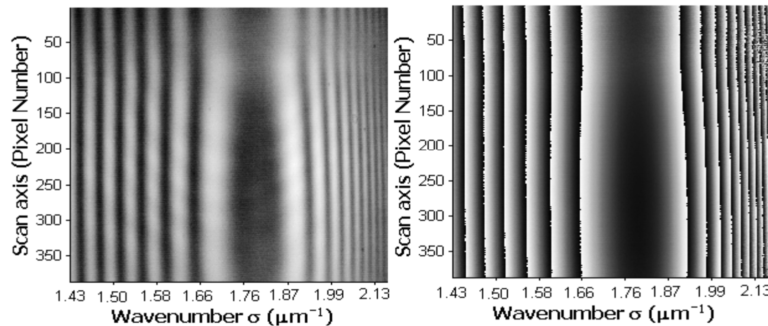

Fig 8. Spectral interferogram of the sample (left) with the corresponding wrapped phase map (right)

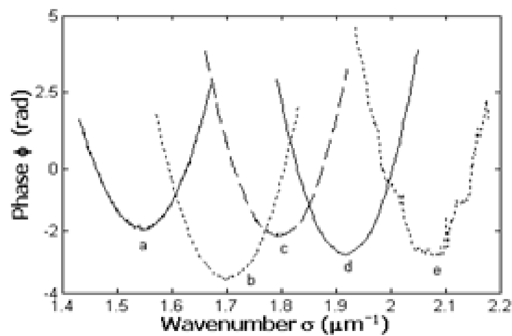

Fig 9. Phase vs. wave number for different stationary pointson calculated curve for silica sample.

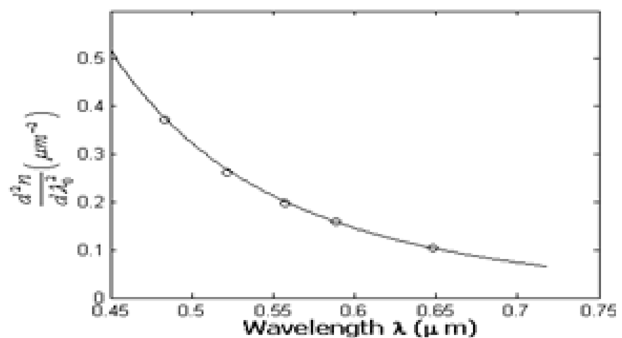

Fig 10. Experimental values(circles) of $d^2n/d\lambda_0^2$

6 Multiple wavelength interferometry

The half a wavelength unambiguous measurement range of monochromatic interferometry is overcome by use of broadband light and spectral interferometry. It is therefore possible to carry out a similar procedure with limited number of wavelengths. Two wavelengths, resulting in larger equivalent wavelength have been used to increase the unambiguous range [29]. Likewise use of three wavelengths has been studied [30-32]. Since the phase vs. wave number relationship is linear, the measurement process involves adding/ subtracting multiples of 2π to the wrapped phase data at the three wavelengths such that the phase vs. wave number graph is linear (Eq (20)). The slope of this line gives a less precise value of the height, which can be refined by the use of Eq (22) as explained earlier. Figure 11 shows a typical result. The profile (a) is by equivalent wavelength method with high noise. The profile (b) is by three wavelengths using fringe order method.

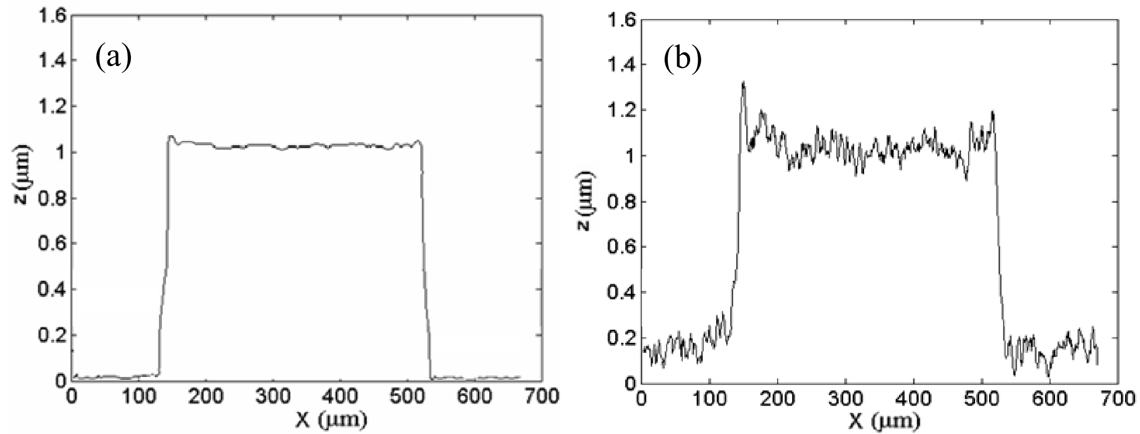

Fig 11. Step profile obtained by multiple wavelengths: (a) three wavelength, (b) two wavelengths. z = 1.125μm.

6.1 White light interferometry with colour CCD camera

The two or three wavelengths used above are usually provided by lasers. An alternate approach would be to record a white light interferogram on three-chip color CCD or a simple color CCD camera. In a three-chip color CCD, signals corresponding to the three wavelengths are provided by the three chips [30]. In a color CCD the signals are obtained from the three color channels of the camera [30,32-34]. Figure 12 shows schematic of white light interferometer with color CCD. The white light fringe pattern and its analysis is represented in Fig 13. This arrangement provides all the color frames in one go. Single shot fringe analysis procedure such as Hilbert transform method can be applied [34,35]. Figure 14 shows 3D profile of a step obtained with color CCD.

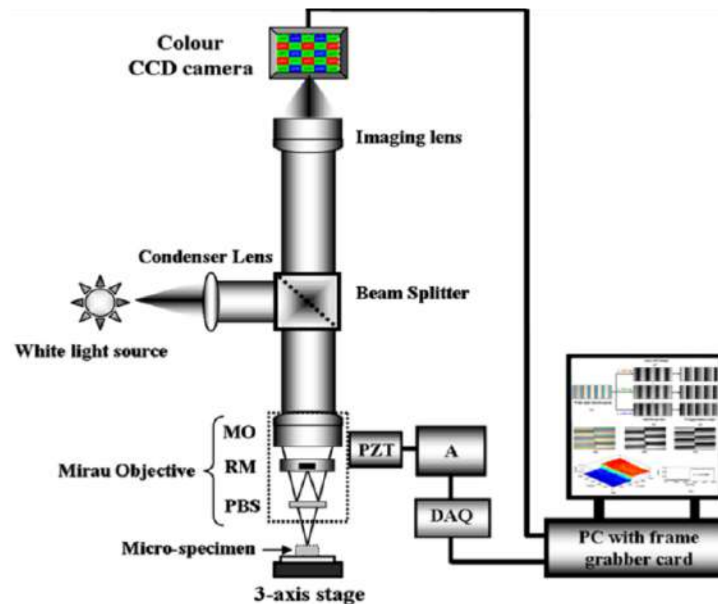

Fig 12. White light interferometer with color CCD

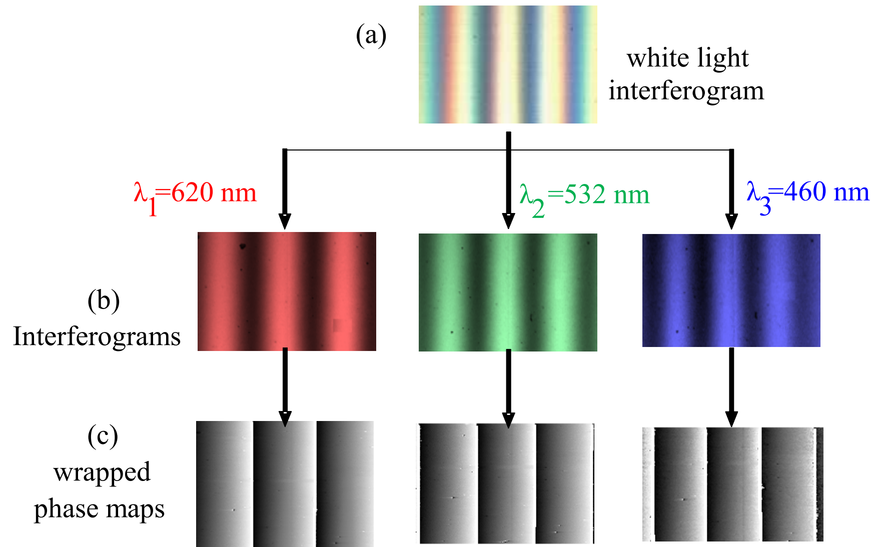

Fig 13. Analyzing a white light interferogram in three-color channels.

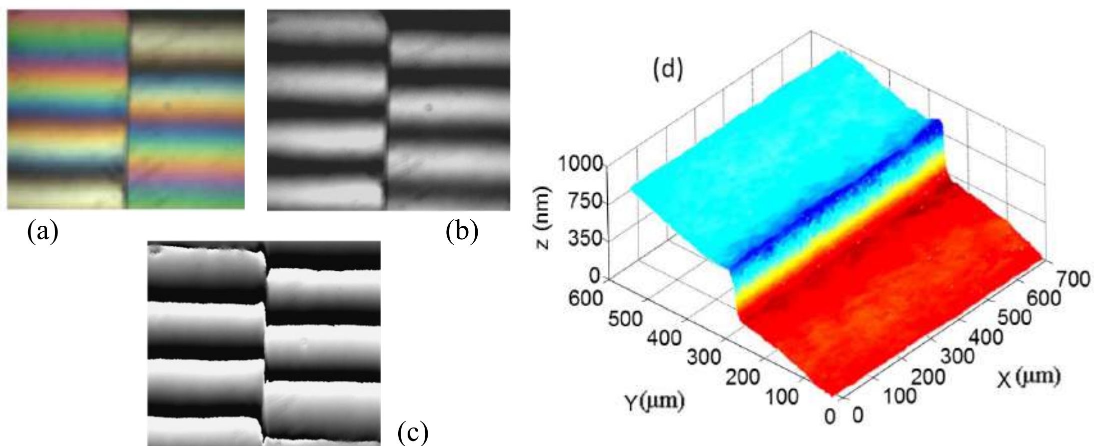

Fig 14. Large step-height analysis using the fringe order method: (a) white light interferogram, (b) interferogram at λ_1, and (c) wrapped phase at λ_1 calculated using Hilbert transformation, and (d) total 3-D surface profile, of an etched silicon sample showing a step of height ~770 nm.

7 Optical coherence tomography

The vertical scanning interferometry with low coherence light makes use of discrete steps to scan the reference or object beam to produce 3D imaging. The property of interferometric localization can be used to carry out 3D imaging by combination of scanning in lateral and axial directions [36]. The scanning in the axial direction is continuous. The technique is known as Optical Coherence Tomography (OCT) and is suitable for imaging /profiling multi-layered structures by measuring the interference signal and depth of each layer boundary. In fact this procedure is called Time Domain OCT. The image is constructed point by point. Figure 15 shows schematic of a fibre optic based OCT arrangement [37]. The detector will produce a

signal that will appear as in Fig 1. Different layers of the medium produce such peaks as the axial scanning is done. The axial distance between the peaks gives the depth information. The axial resolution is determined by the coherence length in the medium and is given by $0.44(\lambda^2/n\Delta\lambda)$, where λ is the wavelength of light, $\Delta\lambda$ the bandwidth and n the refractive index of the medium. Super luminescent light emitting diodes (SLD) commonly used in OCT have $\Delta\lambda \sim 100$nm and at $\lambda \sim 800$nm. With n = 1.3, the resolution is 2µm. This is superior to ultrasonic imaging in which the resolution is of tens of micrometers.

7.1 Spectral domain OCT

If instead of scanning the path difference (z), we vary the frequency (ω) of the light source such as a tunable laser (swept frequency source), the phase will continuously vary (Eq (20)) resulting in a sinusoidal interference signal. The frequency of such a signal is a function of depth (z) [38]. Hence two layers at two different depths will produce different frequencies, which are determined by Fourier transformation.

An alternative to recording the interferogram with swept source, we can use a broadband light source and separate frequency components by a dispersive device at the output as in SRWLI (Fig 3). Now the frequency of the signal along the chromaticity axis is a measure of z.

7.2 Applications of OCT

OCT is a powerful no contact, noninvasive low power optical imaging technique in clinical medicine, particularly ophthalmology. It has also found use in nondestructive testing (NDT) [36].

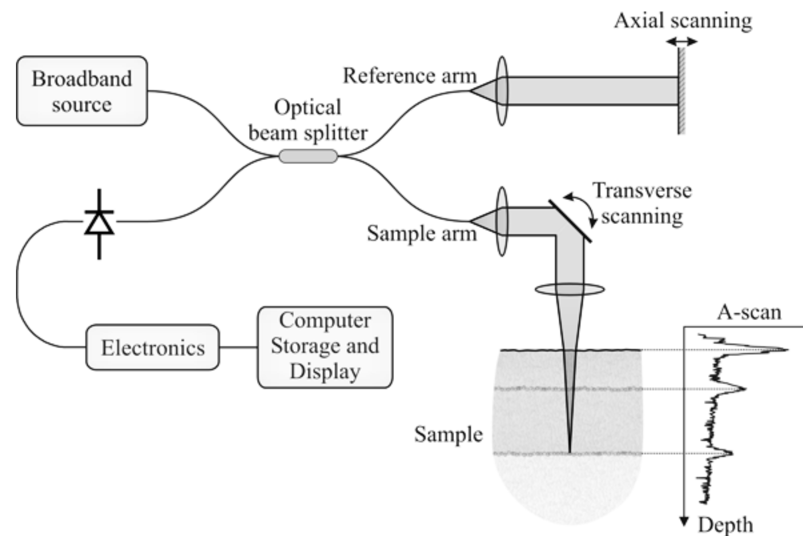

Fig 15. Schematic of a OCT arrangement [Sourced from ref 37] .

8 Femto second laser: A broadband light source for long distance metrology

A femto second (fs) laser is a rich source of optical frequencies that are stable, equally spaced with convenient frequency difference in GHz range. Figure16 shows a femto second laser pulse and its frequency spectrum. The frequency spread covers the entire visible spectrum as seen from the colors of vertical bars in the frequency domain, a frequency comb, representing different frequencies. Effectively it is a broadband light source with short coherence length and has been used for absolute measurement of long length with high precision. Such measurements are of interest in modern experiments such as LIGO and combine spectral interferometry with time of flight method and synthetic wavelength interferometry [39].

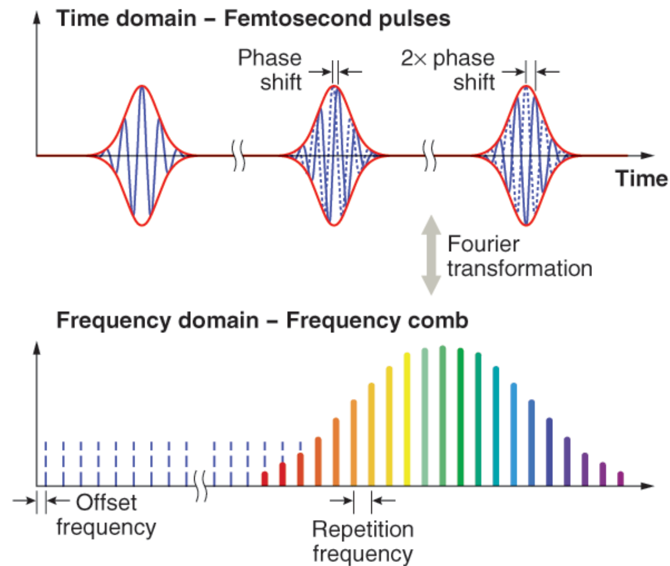

Fig16. A train of femto second pulses and their frequency spectrum [sourced from NIS website]

9 Conclusions

This paper reviews recent applications of broadband light sources. A broadband light source can be a conventional white light such as incandescent lamp or modern light sources such as LED, super luminescent LED, a femto second laser or a superposition of several laser wavelengths resulting in generation of large synthetic wavelength. Absolute measurement is an important characteristics of broadband light as against half a wavelength ambiguity of monochromatic light measurement. Measurements with broadband light are likely to play important role in variety of measurement and testing applications.

References

1. Lee B S, Strand T C, Profilometry with a coherence scanning microscope, *Appl Opt*, 29(1990)3784-3788.
2. Dresel T, HäuslerG,Venzke H, Three dimensional sensing of rough surfaces by coherence radar, *Appl Opt*, 31 (1992)919-925.
3. Caber P J, Interferometric profiler for rough surfaces, *Appl Opt*, 32(1993)3438-3441.
4. Sandoz P, Tribillon G, Profilometry by zero order interference fringe identification, *J Mod Opt*, 40(1993)1691-1700.
5. de Groot P, de Lega X C, Kramer J, Turzhitsky M, Determination of fringe order in White-Light interference microscopy, *Appl Opt*, 41(2002)4571-4578.
6. Sandoz P, Devillers R, Plata A, Unambiguous profilometry by fringe-order identification in white-light phase-shifting interferometry, *J Mod Opt*, 44(1997)519-534.
7. Harasaki A, Schmit J, Wyant C, Improved vertical-scanning interferometry, *Appl Opt*, 39(2000)2107-2115.
8. Greivenkamp J E, Bruning J H, Phase Shifting Interferometers, in *Optical Shop Testing*, 2nd edn, Malacara D (ed), (John Wiley. Sons Inc., New York), 1992, Chapter 14.
9. Kino G S, Chim S C, Mirau correlation microscope, *Appl Opt*, 29(1990)3775-3783.
10. Larkin K G, Efficient nonlinear algorithm for envelope detection in white light interferometry, *J Opt Soc Am A*, 13(1996)832-843.
11. de Groot P, DeckL, Surface profiling by analysis of white light interferograms in the spatial frequency domain, *J Mod Opt*, 42(1995)389-401.

12. Sandoz P, An algorithm for profilometry by white light phase shifting interferometry, *J Mod Opt*, 43(1996) 1545--1554.
13. Suja Helen S, Kothiyal M P, Sirohi R S, Phase shifting by a rotating polarizer in white-light interferometry for surface profiling, *J Mod Opt*, 46(1999)993-1001.
14. Schwider J, Zhou L, Dispersive interferometric profilometer, *Opt Lett*,19(1994)995-997.
15. Pfortner A, Schwider J, Dispersion error in white-light Linnik interferometers and its implications for evaluation procedures, *Appl Opt*, 40(2001)6223-6228.
16. Sandoz P, Tribillon G, Perrin H, High resolution profilometry by using phase calculation algorithms for spectroscopic analysis of white light interferograms, *J Mod Opt*, 43(1996)701-708.
17. Calatroni J, Guerrero A L, Sainz C, EscalonaR, Spectrally resolved white-light interferometry as a profilometry tool, *Opt Laser Tech*, 28(1996)485-489.
18. Suja Helen S, Kothiyal M P, Sirohi R S, Analysis of spectrally resolved white light interferograms: use of a phase shifting technique, *Opt Eng*, 40(2001)1329-1336.
19. Debnath S K, Kothiyal M P, Optical Profiler based on spectrally resolved white light interferometry, *Opt Eng*, 44 (2005)013606-.
20. Debnath S K, Kothiyal M P, Improved optical profiling using spectral phase in spectrally resolved white light interferometry, *Appl Opt*, 45(2006)6965-6972.
21. Kim S W, KimG H, Thickness profile measurement of transparent thin-film layers by white–light scanning interferometry, *Appl Opt*, 38(1999)5968-5973.
22. Debnath S K, Kothiyal M P, Schmit J, Hariharan P, Spectrally resolved white–light phase shifting interference microscopy for thickness–profile measurements of transparent thin – film layers on patterned substrates, *Opt Express*, 14(2006)4662-4667.
23. Debnath S K, Nirmal K V, Kothiyal M P, Spectrally-resolved phase-shifting interferometry for accurate group velocity dispersion measurements, *Opt Lett,* 31(2006)3098-3100.
24. Schmit J, Creath K, Extended averaging technique for derivation of error-compensating algorithms in phase-shifting interferometry, *Appl Opt*, 34(1995)3610-3619.
25. Hariharan P, Oreb B F, Eiju T, Digital phase-shifting interferometer: a simple error-compensating phase calculation algorithm, *Appl Opt*, 26(1987)2504-2506.
26. Sainz C, Calatroni J E, Tribillon G, Refractometry of liquid samples with spectrally resolved white light interferometry, *Meas Sci Tech*, 1(1990)356-361.
27. Sainz C, Jourdain P, Escalona R,Tribillon G, Realtimeinterferometric measurement of dispersion curves, *Opt Commun*, 110(1994)381-390.
28. P Hlubina, White light spectral interferometry to measure effective thickness of optical elements of known dispersion, *Acta Physics Slovaca*, 55(2005)387-393.
29. Cheng Y Y, WyantJ C, Two wavelength phase shifting interferometry, *Appl Opt*, 24(1984)4539-4543.
30. Pfortner A, Schwider J, Red-blue green interferometer for the metrology of discontinuous structures, *Appl Opt,* 42 (2003)667-673.
31. Upputuri P K, Krishna Mohan N, Kothiyal M P**,** Measurement of discontinuous surfaces using multiple-wavelength interferometry, *Opt Eng*, 48(2009)073603-1-073603-8.
32. Upputuri P K, Krishna Mohan N, Kothiyal M P, Red-Green-Blue wavelength Interferometry and TV holography for surface metrology, *J Opt*, 40(2011)176-183.
33. Upputuri P K, Haifeng W, Krishna Mohan N, Kothiyal M P, White light Interferometry for surface profiling with colour CCD, *Opt Lasers Eng*, 50(2012)1084-1088.
34. Upputuri P K, Li G, Haifeng W, Pramanik M, Krishna Mohan N, Kothiyal M P, Measurement of large discontinuities using single white light interferogram, *Opt Express*, 22(2014)27373-27380.
35. Upputuri P K, Manojit Pramanik, Kothiyal M P, Krishna Mohan N, White light single-shot interferometry with

36. Saleh B, *Introduction to subsurface imaging*, (Cambridge University Press), 2011.
37. http://obel.ee.uwa.edu.au/research/oct/intro/
38. Takeda M, Yamamoto H, Fourier transform speckle interferometry: three-dimensional shape measurements of diffuse objects with large height steps and or isolated surfaces, *Appl Opt*, 33(1994)7829-7837.
39. Ki-Nam Joo, Kim Y, Kim S W, Distance measurements by combined method based on a femtosecond pulse laser, *Opt Exp*, 16(2008)19799-19806.

[*Received*: 22.06.2015; *accepted*: 20.7.2015]

M P Kothiyal till recently was professor in the department of physics at IIT Madras. He received his M Tech degree in Applied Optics from IIT Delhi in 1968 and Ph D degree from IIT Madras in 1977. In the period from 1970 to 2014 he held various faculty positions at IIT Madras. His research interests include Optical Instrumentation and Testing, Optical Metrology, Interferometry, and Holography and Speckle techniques. During his research career M P Kothiyal has published over 115 papers in peer reviewed journals and over 100 papers in conference proceedings. He has also coauthored a book. As a DAAD Fellow he carried out research in Germany for about 3 years on different occasions at Institute of Optics, Stuttgart University. He was also a Research Associate at the Centre for Optics and Photonics, Laval University, Canada for two years. M P Kothiyal is a fellow of SPIE-The international society for optical engineering and the Optical Society of America (OSA). He is a joint recipient of NRDC meritorious invention award (2003), and is on the editorial board of Journal of Optics and Asian Journal of Physics (2015)

Paul Kumar Upputuri obtained his M Sc (Physics) degree from Andhra University, Waltair, in 2005, and his Ph D degree from Indian Institute of Technology Madras in 2010. He is currently a Research fellow in the School of Chemical and Biomedical Engineering at Nanyang Technological University. His main research interests are Biomedical Imaging, Photoacoustics, Coherent Raman microscopy, Optical imaging, instrumentation, and metrology. He has published around 60 papers in journals and conference proceedings. He is a member of SPIE, OSA, Indian Laser Association (ILA) and Optical Society of India (OSI).